Changes in work function due to NO_2 adsorption on monolayer and bilayer epitaxial graphene on SiC(0001)

Nuala M. Caffrey,[1,*] Rickard Armiento,[1] Rositsa Yakimova,[1] and Igor A. Abrikosov[1,2,3]
[1]*Department of Physics, Chemistry and Biology (IFM), Linköping University, SE-581 83 Linköping, Sweden*
[2]*Materials Modeling and Development Laboratory, NUST "MISIS," 119049 Moscow, Russia*
[3]*LACOMAS Laboratory, Tomsk State University, 634050 Tomsk, Russia*
(Received 11 August 2016; published 10 November 2016)

The electronic properties of monolayer graphene grown epitaxially on SiC(0001) are known to be highly sensitive to the presence of NO_2 molecules. The presence of small areas of bilayer graphene, on the other hand, considerably reduces the overall sensitivity of the surface. We investigate how NO_2 molecules interact with monolayer and bilayer graphene, both free-standing and on a SiC(0001) substrate. We show that it is necessary to explicitly include the effect of the substrate in order to reproduce the experimental results. When monolayer graphene is present on SiC, there is a large charge transfer from the interface between the buffer layer and the SiC substrate to the molecule. As a result, the surface work function increases by 0.9 eV after molecular adsorption. A graphene bilayer is more effective at screening this interfacial charge, and so the charge transfer and change in work function after NO_2 adsorption is much smaller.

DOI: 10.1103/PhysRevB.94.205411

I. INTRODUCTION

The unique electronic structure of graphene, consisting of linearly dispersing bands around the Dirac point, make it exceptionally sensitive to the adsorption and desorption of molecules which modify its charge carrier density. This, combined with its two-dimensional nature and high carrier mobility, make it an ideal candidate for gas sensing applications. Resistance measurements provide a highly sensitive means of determining the presence of molecular adsorbants on a graphene surface. Ensuring selectivity towards a particular molecule is more challenging, but can be achieved by functionalizing the surface with metallic dopants [1,2] or by analyzing the low-frequency noise after molecular adsorption [3]. Graphene-based NO_2 sensors have been shown to detect concentrations below 1 part per billion (ppb) [4,5]. This ability is imperative as frequent exposure to NO_2 concentrations above the air quality standard of 53 ppb can cause severe damage to the human respiratory system.

While the highest carrier mobilities have been found for suspended graphene samples, they are generally not well suited to device applications. Instead, graphene must be either grown or deposited on a supporting substrate—ideally one that is compatible with Si-based technologies, such as SiO_2 or SiC. However, the interaction between graphene and a substrate can have a significant influence on both the structural and electronic properties of graphene and any material adsorbed or deposited on it [6,7]. The choice of substrate has already been shown to determine the adsorption site of single transition metal adatoms deposited on graphene, and hence their electronic and magnetic properties [8]. If the substrate also plays an important role in the interaction between more weakly interacting molecules and graphene, it could have important implications for graphene-based gas sensors.

The thermal decomposition of SiC(0001) is one of the most promising methods of producing graphene on a scale required for industrial applications. At sufficiently high temperatures, Si atoms sublimate from the surface, leaving behind a carbon-rich surface which undergoes graphitization. The first carbon layer to form is covalently bonded to the SiC substrate, and does not display the electronic features characteristic of graphene. Subsequent carbon layers are strongly *n* doped due to the influence of this carbon buffer layer [9,10,10,11]. There have been several successful experimental studies of using graphene grown on SiC as a NO_2 sensor [3,4,12–16]. At sufficiently high concentrations of NO_2, an *n* to *p* type shift of the graphene layer was found [4,12,14]. The influence of the substrate on the sensing capability of the graphene surface has also being investigated experimentally. Iezhokin *et al.* showed that, by intercalating hydrogen atoms at the interface between SiC and graphene and thereby decoupling the buffer layer, a sixfold increase in the sensitivity of graphene to NO_2 was achieved [7]. However, it is not clear how much of this increased sensitivity is due to the changing electronic interaction at the interface, and how much is due to the unavoidable increase in defects in the decoupled graphene layer.

A further complication is introduced by the presence of different graphene thicknesses on the SiC surface. Although improvements are constantly being achieved in this area, most epitaxial graphene samples contain up to 5% bilayer coverage on an otherwise uniform monolayer sample [15]. This can have unintended consequences on the efficiency of the sensing device. Several experimental studies have attempted to elucidate the difference in response between monolayer and bilayer graphene on SiC when exposed to NO_2 and found that the presence of bilayer graphene significantly reduces the sensitivity of their devices [17,18].

Theoretical studies have shown that NO_2 behaves as a strong charge acceptor when adsorbed on free-standing monolayer graphene [19–21], in agreement with experiment. However, the effect of the substrate and the origin of the thickness dependent sensitivity have not been explicitly considered. Here, we determine the interaction between NO_2

*caffreyn@tcd.ie

 ©2016 American Physical Society

molecules and both free-standing monolayer graphene and monolayer graphene on a SiC(0001) substrate. We show how the graphene reactivity depends on the presence of the substrate and that agreement with experiment can only be achieved by including its effect. We also examine the differences between monolayer and bilayer graphene with respect to molecular adsorption.

II. METHODOLOGY

Density functional theory (DFT) calculations are performed using VASP-5.3 [22–24]. The Perdew-Burke-Ernzerhof (PBE) [25] generalized gradient approximation (GGA) is employed. The DFT-D3 Grimme method [26] is used to include van der Waals interactions. The plane wave basis set is converged using an 800 eV energy cutoff. Structural relaxations of the cell are carried out using a $9 \times 9 \times 1$ k-point Monkhorst-Pack mesh [27] to sample the three-dimensional Brillouin zone. A $21 \times 21 \times 1$ mesh was then used to determine the total energies.

The SiC(0001) substrate is modeled using an asymmetric slab consisting of four bilayers of SiC(0001). The experimentally determined $(6\sqrt{3} \times 6\sqrt{3})R30^\circ$ carbon buffer layer (also known as zero layer graphene or ZLG) [28–31] is modeled using a simplified $\sqrt{3} \times \sqrt{3}R30^\circ$ cell, which has previously been shown to adequately describe the interaction between the SiC substrate and subsequent graphene layers [32–34]. A vacuum layer of at least 17 Å is included in the direction normal to the surface to electronically decouple neighboring slabs and the dipole correction is applied [35,36]. The dangling C bonds on the SiC(000$\bar{1}$) surface are passivated with H atoms. The positions of the top two bilayers of SiC(0001), as well as the H-terminating atoms, the molecular atoms, and all carbon layers, are optimized until all residual forces are less than 0.01 eV Å^{-1}. The remaining atoms are held fixed at their bulk positions.

We consider the adsorption of a NO_2 molecule on both free-standing monolayer and bilayer graphene as well as monolayer and bilayer graphene on SiC(0001) using a 2×2 unit cell. In the following, we refer to free-standing monolayer and bilayer graphene as 1LG and 2LG, respectively, and monolayer and bilayer graphene on SiC(0001) as 1LG/SiC and 2LG/SiC, respectively. Furthermore, we assume the free-standing graphene layers have the same in-plane strain as they have on SiC, in order to eliminate all differences that originate in changing the strain. We choose a very dense concentration of molecules, corresponding to one NO_2 molecule on a 2×2 graphene sheet, i.e., one NO_2 molecule per eight surface carbon atoms, in order to determine whether or not NO_2 is alone capable of generating the n-p transition observed in graphene [12,14].

III. RESULTS

In the following section, we discuss our results for NO_2 adsorbed on 1LG, 1LG/SiC, 2LG, and 2LG/SiC in turn.

A. Free-standing monolayer

In agreement with previous DFT calculations, we find that the energetically favorable configuration of NO_2 on 1LG is that of cycloaddition, i.e., bonding via both oxygen ends, on a bridge site [19,37]. It is adsorbed at an average height of 3.34 Å from the graphene plane [38]. The adsorption energy E_a is calculated as

$$E_a = E_{\text{comb}} - (E_{\text{sur}} + E_{\text{mol}}), \tag{1}$$

where E_{comb} is the total energy of the combined system, E_{sur} is the energy of the clean surface, and E_{mol} is the energy of an isolated NO_2 molecule. Thus, negative values of E_a imply a stable adsorption. We find an adsorption energy of -108 meV for NO_2 adsorbed on 1LG. The low adsorption energy suggests that NO_2 is physisorbed on the graphene surface, in agreement with Raman spectroscopy experiments [39]. This value is considerably smaller than that extracted from thermal desorption spectra of 0.4 eV [40,41]. The high experimental binding energy could be explained by the existence of defects in the graphene layer [42] or the presence of other, unknown, species on the surface [39]. Another possibility is that ripples or ridges are present on the graphene surface [17,43]. These could introduce an sp^3 character to graphene which would in turn influence the molecular binding strength.

NO_2 is a paramagnetic molecule, with a magnetic moment of $1\mu_B$ in the gas phase. When adsorbed on 1LG, the total moment is reduced to $0.97\mu_B$, with the majority of this located on the molecule itself, and $0.005\mu_B$ located on each of the C atoms directly underneath the molecule. As discussed by Leenaerts *et al.* [44], the change in magnetic moment can be a useful indication of charge transfer. Bader analysis [45] shows that $0.05e$ is transferred from graphene to the molecule. This is in agreement with previous DFT calculations [19] and angle-resolved photoemission spectroscopy (ARPES) experiments showing that NO_2 acts as a strong charge acceptor despite its relatively weak binding to the graphene surface [12]. Crowther *et al.* find that $0.012e$ per C atom is transferred to NO_2 monolayers adsorbed on both sides of an isolated graphene sheet, using a Langmuir adsorption isotherm [39]. This is in good agreement with our calculations which have eight C atoms per unit cell and molecular adsorption on only one side of the graphene layer. We note that the charge transfer per molecule will depend on the NO_2 concentration [44]. We find that $0.09e$ is transferred to an NO_2 molecule adsorbed on a 4×4 graphene supercell, with an associated decrease in the total magnetic moment to $0.92\mu_B$.

Figure 1 shows the planar average of the charge density difference (CDD) across the unit cell due to the adsorbed molecule. The CDD is defined as $\Delta\rho = \rho_{\text{comb}} - (\rho_{\text{sur}} + \rho_{\text{mol}})$, where ρ_{comb}, ρ_{sur}, and ρ_{mol} are the charge densities of the final system, the initial system that includes only the surface, and an isolated NO_2 molecule, respectively. It is clear that the charge redistribution is localized primarily at the interface between graphene and the molecule. When NO_2 is adsorbed on 1LG, charge is extracted from a spatial region just above the graphene layer, corresponding to the π orbital. This charge is transferred to NO_2, and in particular to the oxygen orbitals facing the graphene sheet, with a smaller amount located on the N atom.

Scanning Kelvin probe microscopy (SKPM) experiments have consistently shown that graphene experiences a large shift in surface potential, and hence work function, after molecular adsorption [17,18]. This shift depends on the

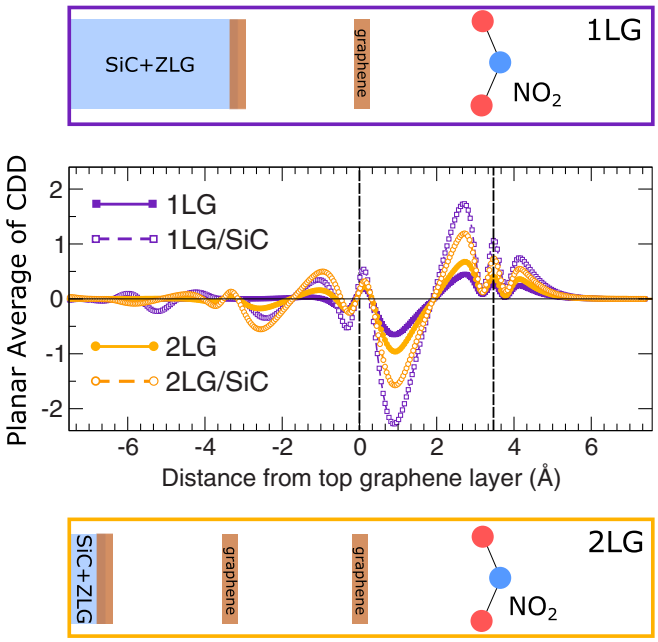

FIG. 1. Middle panel: Planar average of the charge density difference for the 1LG (purple) and 2LG (yellow) systems, both with (open symbols) and without (solid symbols) the SiC substrate. The surface graphene layer is located at 0 Å. Top panel: Schematic of the 1LG structure. Bottom panel: Schematic of the 2LG structure. In both cases, the long axis has the same scale as the middle panel.

graphene thickness, and can be used as a useful tool to estimate the substrate induced doping of graphene layers. The work function, $\Phi = eV_{\text{vacuum}} - E_{\text{F}}$, is obtained by calculating the planar average of the electrostatic potential across the supercell and taking the vacuum potential V_{vacuum} sufficiently far from the surface along the surface normal direction. We find that the work function of 1LG increases by 0.29 eV after NO_2 adsorption, from 5.18 to 5.47 eV.

This modification to the surface work function has two main contributions [46–48]: (i) the intrinsic dipole moment of the molecules, and (ii) an induced interfacial dipole that originates in the charge redistribution after adsorption. It can be written as

$$\Delta\Phi = \Delta V_{\text{mol}} + \Delta\Phi_{\text{bond}}, \tag{2}$$

where ΔV_{mol} is the change in the electrostatic potential across the isolated molecular layer induced by their intrinsic dipole moment and $\Delta\Phi_{\text{bond}}$ is the change in work function induced by a dipole created by the interaction between the molecule and the surface. By definition, this latter term includes contributions from bond formation, charge transfer, structural changes in both the molecule and graphene due to their interaction, dipole image creation, etc. The former term, ΔV_{mol}, can be determined by calculating the step in the planar average of the macroscopic electrostatic potential across the molecular layer, in the same configuration as it is adsorbed on the graphene surface. We find ΔV_{mol} to be -0.37 eV. The magnitude of the associated dipole can be estimated using the

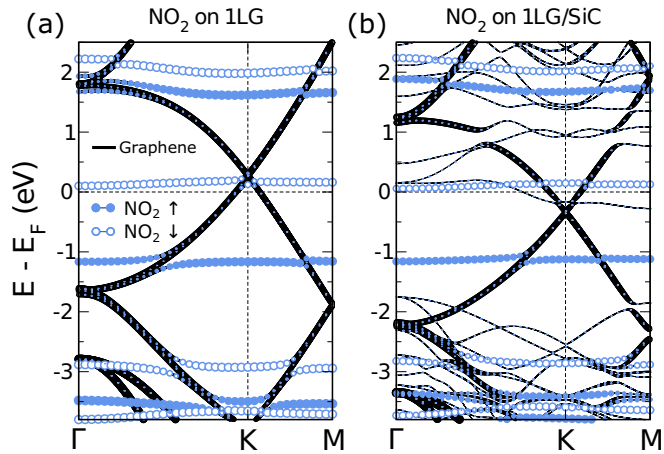

FIG. 2. Electronic structure of (a) the 1LG structure after NO_2 adsorption and (b) the 1LG/SiC structure after NO_2 adsorption. In both cases the in-plane unit cell corresponds to that of 2×2 graphene. The NO_2 and graphene character of the bands has been determined by projecting onto the atomic orbitals of the respective atoms. For bands with graphene character, the band thickness represents the magnitude of the overlap.

Helmholtz equation

$$\Delta V_{\text{mol}} = -\frac{q_e}{\epsilon_0}\frac{\Delta\mu_{\text{mol}}}{A}, \tag{3}$$

where q_e is the electron charge, ϵ_0 is the vacuum permittivity, $\Delta\mu_{\text{mol}}$ is the molecular dipole, and A is the surface area. This corresponds to a dipole moment of 0.24 D directed away from the surface, in reasonable agreement with the experimentally determined NO_2 dipole moment of 0.32 D pointing from the oxygen atoms to the nitrogen atom [49]. We note that at very high molecular concentration, there may be a depolarization effect that reduces the molecular dipole. We find that reducing the concentration of molecules by a factor of 4 reduces the dipole moment by only 0.01 D and so can be neglected. Using Eq. (2), the change in work function that can then be attributed to a charge transfer is 0.65 eV. According to the Helmholtz equation this corresponds to a dipole of 0.43 D pointing towards the surface, as expected from the charge accepting behavior of NO_2, and opposing that of $\Delta\Phi_{\text{mol}}$. Although quite a crude approximation, this dipole moment corresponds to charge transfer Q of $0.05e$ over a distance $\vec{d}$ of 3.34 Å, using $\vec{\mu} = Q\vec{d}$, in good agreement with the charge transfer calculated using the Bader method.

The resulting band structure is shown in Fig. 2(a). The p doping of the graphene layer by NO_2 is evident by the position of the Dirac point 0.28 eV above the Fermi level. A Fermi level shift of 0.83 eV was measured using ARPES when NO_2 was adsorbed on both sides of a free-standing graphene sheet [39]. If we assume the two molecular layers do not interact, it is a reasonable assumption that a single molecular layer will shift the Fermi level by 0.42 eV, in relatively good agreement with the theoretical result. The lowest unoccupied molecular orbital (LUMO) is pinned at the Fermi level and is negatively spin polarized. The corresponding spin-split orbital comprises the highest occupied molecular orbital (HOMO) and can be found 1.2 eV below the Fermi level, in agreement with Ref. [19].

Dimers

It is possible that both monomers and dimers of NO_2 are present on the graphene surface [20]. We find that the most energetically favorable orientation of a dimer on graphene is that with the molecular plane, and N = N bond, normal to the surface. This is very similar to the experimentally determined geometry of NO_2 dimers on graphite [40,50]. The N_2O_4 molecules interact only very weakly with the surface, with a charge transfer of $0.01e$ from graphene to the molecule. The work function of the surface increases to 5.00 eV after dimer adsorption; this should be compared to 5.18 eV after monomer adsorption. In agreement with Ref. [20], we find that the HOMO of the dimer is located 2.6 eV below the Dirac point and so does not facilitate any doping of the graphene layer. This is corroborated by the calculated band structure, which positions the Dirac point at the Fermi level (not shown). From this we can conclude that the creation of N_2O_4 on the surface cannot account for the switch to p doping of graphene when exposed to NO_2.

B. Monolayer on SiC

We now consider how the interaction of the graphene monolayer with a SiC substrate affects the reactivity of this surface to an NO_2 molecule. We first note that SiC does not influence the binding position or binding height of the molecule from the graphene layer. Despite this, the adsorption energy increases dramatically from −108 to −154 meV. The work function also increases compared to that of NO_2 on 1LG, by 0.14 eV, to 5.32 eV. Given that the intrinsic molecular moment has not changed, this increase in work function must be driven by an increased charge transfer when the SiC substrate is present [see Eq. (2)]. Indeed, Bader analysis shows that $0.08e$ is transferred from graphene to the molecule, compared to $0.05e$ on 1LG. The increase in charge transfer is also evident by the decrease in the molecular magnetic moment, from $0.97\mu_B$ to $0.90\ \mu_B$. The influence of the SiC substrate on the charge transferred to the molecule can be seen in Fig. 1. Compared to the case of NO_2 on free-standing graphene, it is clear that there is a dramatic increase in the magnitude of charge transfer when the SiC substrate is taken into account.

The clean graphene layer on SiC is strongly n doped, with the experimental Dirac point located 0.45 eV below the Fermi level [10]. The band structure associated with NO_2 adsorbed on this 1LG/SiC surface is shown in Fig. 2(b). The Dirac point is now shifted 0.24 eV back towards the Fermi level, i.e., by an amount very similar to that on free-standing graphene. Nonetheless, the Dirac point remains below the Fermi level; it appears that even at this high concentration, the adsorption of NO_2 on 1LG/SiC cannot account for the n-p transition observed experimentally. We note, however, that for the sample considered in Ref. [12] where an n-p transition was observed, the Dirac point for the clean surface was located only 0.3 eV below the Fermi level. In this case, an n-p transition is more likely with a sufficiently high concentration of adsorbed NO_2. Details of the differing reaction of 1LG and 1LG/SiC to the presence of NO_2 molecules are summarized in Table I.

TABLE I. Surface work function (Φ) before and after NO_2 adsorption both for a free-standing graphene monolayer and for an epitaxial graphene monolayer on SiC. Adsorption energy (E_a) of NO_2 molecules on graphene for the same structures.

		Φ (eV)	E_a (meV)
With NO_2			
	NO_2/1 ML	5.18	−108
	NO_2/1 ML/SiC	5.32	−154
Without NO_2			
	1 ML	4.89	
	1 ML/SiC	4.42	

C. Free-standing bilayer

We now consider the interaction between NO_2 and free-standing bilayer graphene (2LG). As NO_2 is not found to intercalate between the two graphene layers at low values of temperature and pressure [39], we consider here only adsorption on one side of the bilayer.

The binding energy of NO_2 on 2LG is found to be −114 meV, a value very similar to that on 1LG (−108 meV). Similarly, the total magnetic moment of the system is 0.98 μ_B, close to that found on 1LG, which would suggest that the same amount of charge is transferred from 2LG to NO_2. This is reflected in the Bader charges which show that $0.05e$ is transferred from 2LG to NO_2. The majority of this charge ($0.04e$) is transferred from the graphene layer nearest the molecule. This is shown more clearly in Fig. 1. When NO_2 is adsorbed on a 2LG, the magnitude of the charge transfer is slightly greater compared to when it adsorbs on 1LG. The charge rearrangement on the lower graphene layer, i.e., the one not in contact with the NO_2 molecule, is smaller. Combined, these results suggest that 1LG and 2LG have a very similar reactivity to NO_2. As a result, the work function of bilayer graphene after NO_2 adsorption is the same as that for monolayer graphene—an increase of approximately 0.26 eV over the clean 2LG surface.

The band structure is shown in Fig. 3(a). The Dirac point after NO_2 adsorption is found to be located 0.18 eV above the Fermi level. This shift is smaller than that found after adsorption on 1LG (0.28 eV). Furthermore, a small band gap of approximately 80 meV opens due to the asymmetric doping of the bilayer by the NO_2 molecules.

Despite the differing electronic structure of 1LG and 2LG close to the Fermi level, namely, linear dispersion compared to parabolic dispersion, the interaction with NO_2 is very similar. Yet experiment has generally found that monolayer graphene on SiC has a considerably higher reactivity than bilayer graphene. We discuss next how the interaction of bilayer graphene with the SiC substrate changes its interaction with NO_2.

D. Bilayer on SiC

SKPM measurements have shown that 2LG/SiC exhibits a smaller shift in surface potential, and hence work function, upon exposure to NO_2 that 1LG/SiC [17,18]. We calculate a work function of 5.26 eV when NO_2 is adsorbed on 2LG/SiC,

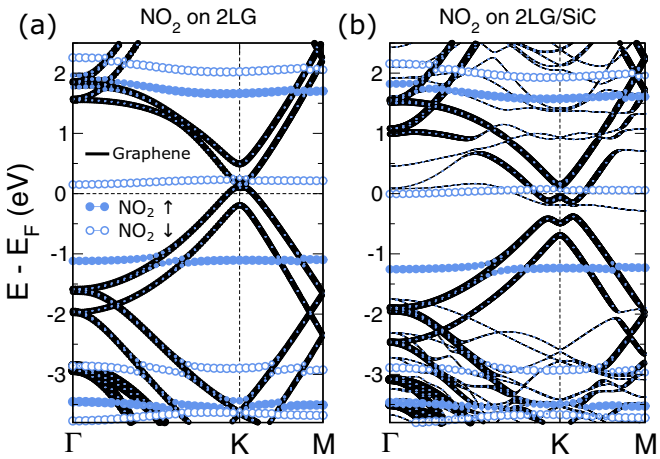

FIG. 3. Electronic structure of (a) the free-standing 2LG structure after NO_2 adsorption and (b) the 2LG/SiC structure after NO_2 adsorption. As in Fig. 2, the NO_2 and graphene character of the bands has been determined by projecting onto the atomic orbitals of the respective atoms. For bands with graphene character, the band thickness represents the magnitude of the overlap.

i.e., an increase of 0.64 eV over the clean surface. In agreement with experiment, we find that this is a smaller change compared to 1LG/SiC where the change in work function after NO_2 adsorption is 0.91 eV. As the intrinsic dipole associated with the adsorbed molecules is the same for those adsorbed on 1LG/SiC and 2LG/SiC at the same concentration, the change in work function must be related entirely to the reduced charge transfer found for the 2LG/SiC system compared to the 1LG/SiC system. This can be seen in Fig. 1. The top carbon layer screens the charge associated with the ZLG/SiC interface, thereby reducing the electrostatic interaction between the molecules and the surface. As a result, the effectiveness of the molecular interaction on 2LG/SiC is reduced compared to 1LG/SiC.

Experiment has also found that the Fermi level coincides with the charge neutrality point in a shorter time when NO_2 is adsorbed on 2LG/SiC than on 1LG/SiC [18]. This demonstrates a rapid change in the charge carrier concentration for 2LG/SiC. It was suggested that either more NO_2 is adsorbed on 2LG/SiC than on 1LG/SiC or that 2LG/SiC transfers more charge to NO_2 than 1LG/SiC. To address the former, we determined the binding energy of NO_2 on the 2LG/SiC surface to be -0.132 eV, a decrease of 22 meV compared to the 1LG/SiC case. This would make it unlikely that more NO_2 is adsorbed on the 2LG/SiC surface. As for the latter, we have shown that the charge transfer from NO_2 is greater for the 1LG/SiC case. A third possibility could be that the combined effect of substrate and molecular doping introduces a large asymmetry across the graphene bilayer. This would open a sizable band gap which could result in the system reaching the charge neutrality point quicker for the 2LG/SiC system. To address this, we show the band structure associated with this configuration in Fig. 3(b). The effect of NO_2 on the clean 2LG/SiC system is to shift the Dirac point by 0.19 eV closer to the Fermi energy. This is a slightly smaller shift compared to that induced by NO_2 on 1LG/SiC, which shifts the position of the Dirac point by 0.24 eV. However, the asymmetry induced by both the SiC substrate and the adsorbed molecules on the bilayer of graphene is very evident in the large band gap of 0.24 eV that opens at the Dirac point and the associated "wizard hat" structure. In comparison, the gap that opens due to the asymmetry introduced by the molecules alone is 0.08 eV. A summary of the results related to the interaction between NO_2 and bilayer graphene is given in Table II.

TABLE II. Surface work function (Φ) before and after NO_2 adsorption both for a free-standing graphene bilayer and for an epitaxial graphene bilayer on SiC. Adsorption energy (E_a) of NO_2 molecules on graphene for the same structures.

		Φ (eV)	E_a (meV)
With NO_2			
	NO_2/2 ML	5.18	-114
	NO_2/2 ML/SiC	5.26	-132
Without NO_2			
	2 ML	4.92	
	2 ML/SiC	4.62	

IV. CONCLUSIONS

In conclusion, we investigated how NO_2 molecules interact with monolayer and bilayer graphene, both free-standing and on a SiC(0001) substrate. We demonstrate that explicitly including the substrate is necessary in order to reproduce experimental results. We find that the presence of NO_2 increases the work function by approximately 0.3 eV for both free-standing monolayer and bilayer graphene. When the SiC substrate is included, NO_2 increases the work function by 0.9 eV when adsorbed on monolayer graphene but only by 0.64 eV on bilayer graphene. This can be related to the increase in charge transferred to the molecule from the substrate. This increased charge transfer results in a large induced dipole and hence an increase in work function. As the bilayer system is more efficient at screening the buildup of charge at the interface, the induced dipole due to charge transfer is smaller. Therefore, we find that the large reactivity of the monolayer graphene to NO_2 is due to the effect of the SiC substrate. Any investigation of NO_2 gas sensors based on graphene grown on SiC must take the effect of the substrate into account.

ACKNOWLEDGMENTS

This project has received funding from the European Union's Horizon 2020 research and innovation programme under Grant Agreement No. 696656. The authors also wish to acknowledge the Swedish Research Council (VR) Grant No. 621-2014-5805 and the Swedish Foundation for Strategic Research (SSF) program SRL Grant No. 10-0026 and the Swedish Government Strategic Research Area SeRC. R.A. acknowledges financial support from the Linnaeus Environment at Linköping on Nanoscale Functional Materials (LiLi-NFM) funded by VR. I.A.A. acknowledges the support from the Grant of Ministry of Education and Science of the Russian Federation (Grant No. 14.Y26.31.0005) and Tomsk State University Academic D. I. Mendeleev Fund Program

(Project No. 8.1.18.2015). The authors would like to thank Jens Eriksson for useful discussions. All calculations were performed using the supercomputer resources of the Swedish National Infrastructure for Computing (SNIC) at the National Supercomputing Center (NSC) and at the PDC Center for High Performance Computing (PDC-HPC).

[1] B. Cho, J. Yoon, M. G. Hahm, D.-H. Kim, A. R. Kim, Y. H. Kahng, S.-W. Park, Y.-J. Lee, S.-G. Park, J.-D. Kwon *et al.*, Graphene-based gas sensor: Metal decoration effect and application to a flexible device, J. Mater. Chem. C **2**, 5280 (2014).

[2] Z. Zhang, X. Zou, L. Xu, L. Liao, W. Liu, J. Ho, X. Xiao, C. Jiang, and J. Li, Hydrogen gas sensor based on metal oxide nanoparticles decorated graphene transistor, Nanoscale **7**, 10078 (2015).

[3] S. Rumyantsev, G. Liu, M. S. Shur, R. A. Potyrailo, and A. A. Balandin, Selective gas sensing with a single pristine graphene transistor, Nano Lett. **12**, 2294 (2012).

[4] F. Schedin, A. K. Geim, S. V. Morozov, E. W. Hill, P. Blake, M. I. Katsnelson, and K. S. Novoselov, Detection of individual gas molecules adsorbed on graphene, Nat. Mater. **6**, 652 (2007).

[5] W. Yuan and G. Shi, Graphene-based gas sensors, J. Mater. Chem. A **1**, 10078 (2013).

[6] Q. H. Wang, Z. Jin, K. K. Kim, A. J. Hilmer, G. L. C. Paulus, C.-J. Shih, M.-H. Ham, J. D. Sanchez-Yamagishi, K. Watanabe, T. Taniguchi *et al.*, Understanding and controlling the substrate effect on graphene electron-transfer chemistry via reactivity imprint lithography, Nat. Chem. **4**, 724 (2012).

[7] I. Iezhokin, P. Offermans, S. H. Brongersma, A. J. M. Giesbers, and C. F. J. Flipse, High sensitive quasi freestanding epitaxial graphene gas sensor on 6H-SiC, Appl. Phys. Lett. **103**, 053514 (2013).

[8] T. Eelbo, M. Waśniowska, M. Gyamfi, S. Forti, U. Starke, and R. Wiesendanger, Influence of the degree of decoupling of graphene on the properties of transition metal adatoms, Phys. Rev. B **87**, 205443 (2013).

[9] F. Varchon, R. Feng, J. Hass, X. Li, B. N. Nguyen, C. Naud, P. Mallet, J.-Y. Veuillen, C. Berger, E. H. Conrad, and L. Magaud, Electronic Structure of Epitaxial Graphene Layers on SiC: Effect of the Substrate, Phys. Rev. Lett. **99**, 126805 (2007).

[10] C. Riedl, C. Coletti, and U. Starke, Structural and electronic properties of epitaxial graphene on SiC(0001): A review of growth, characterization, transfer doping and hydrogen intercalation, J. Phys. D **43**, 374009 (2010).

[11] K. V. Emtsev, A. Bostwick, K. Horn, J. Jobst, G. L. Kellogg, L. Ley, J. L. McChesney, T. Ohta, S. A. Reshanov, J. Röhrl *et al.*, Towards wafer-size graphene layers by atmospheric pressure graphitization of silicon carbide, Nat. Mater. **8**, 203 (2009).

[12] S. Y. Zhou, D. A. Siegel, A. V. Fedorov, and A. Lanzara, Metal to Insulator Transition in Epitaxial Graphene Induced by Molecular Doping, Phys. Rev. Lett. **101**, 086402 (2008).

[13] M. Qazi, M. W. K. Nomani, M. V. S. Chandrashekhar, V. B. Shields, M. G. Spencer, and G. Koley, Molecular adsorption behavior of epitaxial graphene grown on 6H-SiC faces, Appl. Phys. Express **3**, 075101 (2010).

[14] R. Pearce, T. Iakimov, M. Andersson, L. Hultman, A. L. Spetz, and R. Yakimova, Epitaxially grown graphene based gas sensors for ultra sensitive NO_2 detection, Sens. Actuators, B **155**, 451 (2011).

[15] V. Panchal, R. Pearce, R. Yakimova, A. Tzalenchuk, and O. Kazakova, Standardization of surface potential measurements of graphene domains, Sci. Rep. **3**, 2597 (2013).

[16] S. Novikov, N. Lebedeva, and A. Satrapinski, Ultrasensitive NO_2 gas sensor based on epitaxial graphene, J. Sensors **2015**, 108581 (2015).

[17] R. Pearce, J. Eriksson, T. Iakimov, L. Hultman, A. Lloyd Spetz, and R. Yakimova, On the differing sensitivity to chemical gating of single and double layer epitaxial graphene explored using scanning Kelvin probe microscopy, ACS Nano **7**, 4647 (2013).

[18] R. E. Hill-Pearce, V. Eless, A. Lartsev, N. A. Martin, I. L. Barker Snook, J. J. Helmore, R. Yakimova, J. C. Gallop, and L. Hao, The effect of bilayer regions on the response of epitaxial graphene devices to environmental gating, Carbon **93**, 896 (2015).

[19] O. Leenaerts, B. Partoens, and F. M. Peeters, Adsorption of H_2O, NH_3, CO, NO_2, and NO on graphene: A first-principles study, Phys. Rev. B **77**, 125416 (2008).

[20] T. O. Wehling, K. S. Novoselov, S. V. Morozov, E. E. Vdovin, M. I. Katsnelson, A. K. Geim, and A. I. Lichtenstein, Molecular doping of graphene, Nano Lett. **8**, 173 (2008).

[21] T. O. Wehling, M. I. Katsnelson, and A. I. Lichtenstein, Adsorbates on graphene: Impurity states and electron scattering, Chem. Phys. Lett. **476**, 125 (2009).

[22] G. Kresse and J. Furthmüller, Efficient iterative schemes for *ab initio* total-energy calculations using a plane-wave basis set, Phys. Rev. B **54**, 11169 (1996).

[23] G. Kresse and D. Joubert, From ultrasoft pseudopotentials to the projector augmented-wave method, Phys. Rev. B **59**, 1758 (1999).

[24] P. E. Blöchl, Projector augmented-wave method, Phys. Rev. B **50**, 17953 (1994).

[25] J. P. Perdew, K. Burke, and M. Ernzerhof, Generalized Gradient Approximation Made Simple, Phys. Rev. Lett. **77**, 3865 (1996).

[26] S. Grimme, J. Antony, S. Ehrlich, and H. Krieg, A consistent and accurate *ab initio* parametrization of density functional dispersion correction (DFT-D) for the 94 elements H-Pu, J. Chem. Phys. **132**, 154104 (2010).

[27] H. J. Monkhorst and J. D. Pack, Special points for Brillouin-zone integrations, Phys. Rev. B **13**, 5188 (1976).

[28] F. Owman and P. Mårtensson, The SiC(0001) $6\sqrt{3} \times 6\sqrt{3}$ reconstruction studied with STM and LEED, Surf. Sci. **369**, 126 (1996).

[29] W. Chen, H. Xu, L. Liu, X. Gao, D. Qi, G. Peng, S. C. Tan, Y. Feng, K. P. Loh, and A. T. S. Wee, Atomic structure of the 6H-SiC (0001) nanomesh, Surf. Sci. **596**, 176 (2005).

[30] M.-H. Tsai, C. S. Chang, J. D. Dow, and I. S. T. Tsong, Electronic contributions to scanning-tunneling-microscopy images of an annealed β-SiC(111) surface, Phys. Rev. B **45**, 1327 (1992).

[31] J. Hass, R. Feng, T. Li, X. Li, Z. Zong, W. A. De Heer, P. N. First, E. H. Conrad, C. A. Jeffrey, and C. Berger, Highly ordered graphene for two dimensional electronics, Appl. Phys. Lett. **89**, 143106 (2006).

[32] K. V. Emtsev, F. Speck, Th. Seyller, L. Ley, and J. D. Riley, Interaction, growth, and ordering of epitaxial graphene on SiC (0001) surfaces: A comparative photoelectron spectroscopy study, Phys. Rev. B **77**, 155303 (2008).

[33] N. M. Caffrey, R. Armiento, R. Yakimova, and I. A. Abrikosov, Charge neutrality in epitaxial graphene on 6H-SiC (0001) via nitrogen intercalation, Phys. Rev. B **92**, 081409 (2015).

[34] N. M. Caffrey, L. I. Johansson, C. Xia, R. Armiento, I. A. Abrikosov, and C. Jacobi, Structural and electronic properties of Li-intercalated graphene on SiC (0001), Phys. Rev. B **93**, 195421 (2016).

[35] J. Neugebauer and M. Scheffler, Adsorbate-substrate and adsorbate-adsorbate interactions of Na and K adlayers on Al(111), Phys. Rev. B **46**, 16067 (1992).

[36] G. Makov and M. C. Payne, Periodic boundary conditions in *ab initio* calculations, Phys. Rev. B **51**, 4014 (1995).

[37] Y.-H. Zhang, Y.-B. Chen, K.-G. Zhou, C.-H. Liu, J. Zeng, H. -L. Zhang, and Y. Peng, Improving gas sensing properties of graphene by introducing dopants and defects: A first-principles study, Nanotechnology **20**, 185504 (2009).

[38] The distance from the adsorbate to the graphene surface is calculated from the difference in weighted averages of the different atoms of the molecule and the carbon atoms of the graphene sheet, where we used the atomic number Z of the atoms as the weight factor.

[39] A. C. Crowther, A. Ghassaei, N. Jung, and L. E. Brus, Strong charge-transfer doping of 1 to 10 layer graphene by NO_2, ACS Nano **6**, 1865 (2012).

[40] P. Sjövall, S. K. So, B. Kasemo, R. Franchy, and W. Ho, NO_2 adsorption on graphite at 90 K, Chem. Phys. Lett. **172**, 125 (1990).

[41] H. Ulbricht, R. Zacharia, N. Cindir, and T. Hertel, Thermal desorption of gases and solvents from graphite and carbon nanotube surfaces, Carbon **44**, 2931 (2006).

[42] G. Lee, G. Yang, A. Cho, J. W. Han, and J. Kim, Defect-engineered graphene chemical sensors with ultra-high sensitivity, Phys. Chem. Chem. Phys. **18**, 14198 (2016).

[43] M. I. Katsnelson and A. K. Geim, Electron scattering on microscopic corrugations in graphene, Philos. Trans. R. Soc. London A **366**, 195 (2008).

[44] O. Leenaerts, B. Partoens, and F. M. Peeters, Paramagnetic adsorbates on graphene: A charge transfer analysis, Appl. Phys. Lett. **92**, 243125 (2008).

[45] W. Tang, E. Sanville, and G. Henkelman, A grid-based Bader analysis algorithm without lattice bias, J. Phys.: Condens. Matter **21**, 084204 (2009).

[46] B. de Boer, A. Hadipour, M. M. Mandoc, T. van Woudenbergh, and P. W. M. Blom, Tuning of metal work functions with self-assembled monolayers, Adv. Mater. **17**, 621 (2005).

[47] O. T. Hofmann, D. A. Egger, and E. Zojer, Work-function modification beyond pinning: When do molecular dipoles count?, Nano Lett. **10**, 4369 (2010).

[48] D. Cornil, T. Van Regemorter, D. Beljonne, and J. Cornil, Work function shifts of a zinc oxide surface upon deposition of self-assembled monolayers: A theoretical insight, Phys. Chem. Chem. Phys. **16**, 20887 (2014).

[49] D. R. Lide, *CRC Handbook of Chemistry and Physics* (CRC Press, Boca Raton, FL, 2004), Vol. 85.

[50] R. Moreh, Y. Finkelstein, and H. Shechter, NO_2 adsorption on Grafoil between 297 and 12 K, Phys. Rev. B **53**, 16006 (1996).